PCCP

Electrocatalytic activity of various types of h-BN for oxygen reduction reaction

SCHOLARONE™
Manuscripts

Journal Name

Physical Chemistry Chemical Physics

ARTICLE TYPE

Electrocatalytic activity of various types of h-BN for oxygen reduction reaction

Ganesan Elumalai,[a,b] Hidenori Noguchi,[a,b,c] and Kohei Uosaki[a,b,c*]

5 [a]Graduate School of Chemical Science and Engineering, Hokkaido University, Sapporo 060-0810, Japan

[b]Global Research Center for Environment and Energy based on Nanomaterials Science (GREEN), National Institute for Materials Science (NIMS), Tsukuba 305-0044, Japan

[c]International Center for Materials Nanoarchitectonics (WPI-MANA), National Institute for Materials Science (NIMS), 1-1 Namiki, Tsukuba 305-0044, Japan

Electrocatalytic activities of various types of h-BN, i.e., spin coated BN nanotube (BNNT) and BN nanosheet (BNNS) and sputter deposited BN, on Au electrodes as well as those of BNNS modified glassy carbon (GC) and Pt electrodes for oxygen reduction reaction (ORR) were examined in O_2 saturated 0.5M
15 H_2SO_4 solution based on the theoretical prediction that monolayer BN on metal substrate may act as an electrocatalyst for ORR although bulk BN is an insulator with wide band gap. The overpotential for ORR at Au electrode was reduced by ca. 100, ca. 270, and ca.150 mV by spin coating of the dispersion of BNNT and liquid exfoliated BNNS, and sputter deposition of BN, respectively, proving the theoretical prediction. On the other hand, no change in the overpotential was observed at glassy carbon electrode by
20 the BNNS modification and the overpotential even increased at Pt electrode, suggesting that the interaction between BN and Au plays an important role for BN to become ORR active.

1. Introduction

Electrocatalysts for oxygen reduction reaction (ORR) have been studied for long time because high overpotential for ORR is one
25 of the most preventing factors for the wide spread use of fuel cell.[1-4] Because of high cost, less abundance, low stability and still sluggish kinetics of Pt based electrocatalyst, which is currently the best electrocatalyst for ORR, many research groups are making efforts to find non-precious metal electrocatalysts
30 such as non−precious metals,[5-13] their alloys, metal oxides,[14] metal nitrides,[15,16] metal oxynitrides,[17,18] metal carbides[16,19]as well as N- and B-doped carbon materials with and without metal doping.[20-24] While the enhanced catalytic activity of N-doped carbon for ORR was attributed to the electron accepting behavior
35 of nitrogen species, which creates a net positive charge on neighboring carbon atoms, where O_2 adsorbed,[24,25] O_2 is considered to be adsorbed on boron atom itself in the case of B-doped carbon due to electron accepting behavior of B atom.[26] B- and N- co-doped carbon showed higher ORR activity[26-28] and it
40 was considered that B atoms stabilize the N impurity near the edge of the graphene cluster and make it more reactive.[28]

If all the carbon atoms of graphene are substituted by B- and N-atoms, hexagonal boron nitride (h-BN) monolayer, which has geometric structure similar to graphene, can be obtained.[29] Since

45 BN is an insulator with a wide band gap (3.6-7.1eV depending on the experimental methods)[30-32] and is known to be chemically inert,[33,34] one would not expect BN to be a good electrocatalyst for ORR. It has been reported, however, that the band gap energy of BN can be modulated by B- and N- vacancies and impurity
50 defects[35,36] and atomically thin h-BN nanoribbon is semi-conducting due to edge states and vacancy defects.[35] Thus, ultrathin BN layers supported on conducting material can be a candidate for ORR electrocatalyst. Actually, we have recently demonstrated that an inert h-BN monolayer can be functionalized
55 and become catalytically active by nitrogen doping[37] and by the metal (Ni(111)) support[38] and readily bind to transition metal surfaces due to the mixing of the d_z^2 metal orbitals with the N-p_z and B-p_z orbitals of h-BN,[39] which is responsible for considerable modifications of the electronic properties of h-BN monolayer
60 supported on 3d, 4d, and 5d transition metal surfaces[40,41]and the catalytic activity of small metal particles supported on h-BN.[40-42]More recently, we have communicated that h-BN nannosheet supported on Au is a good electrocatalyst for ORR based both on DFT calculations and experimental results. The importance of the
65 interaction between Au substrate and BN was suggested.

In this study, we have investigated electrocatalytic activities of various types of h-BN on Au, i.e., spin coated BN nanotube (BNNT) and BN nanosheet (BNNS) and sputter deposited BN, in

O_2 saturated 0.5M H_2SO_4 solution. Electrocatalytic activities of BNNS modified glassy carbon (GC) and Pt electrodes are also examined to clarify the role of substrate.

2. Experimental

2.1 Materials

Ultrapure reagent grade H_2SO_4, isopropyl alcohol (IPA), and acetone were purchased from Wako Pure Chemicals. Water was purified using a Milli-Q system (Yamato, WQ-500). Boron Nitride (BN) powder (99%) was purchased from High Purity Chemicals (BBIO3PB4). n-Si(111) wafers (P-doped, resistivity of 1-10Ω) were donated by Shin-Etsu Semiconductor. GC (10x10x1mm) was purchased from BAS (No. 012825).

2.2 Sample preparation

Au and Pt substrates were prepared on n-Si(111), which was precleaned by sonication in acetone and Milli-Q water about 5min each and then thoroughly washed with conc. sulfuric acid and Milli-Q water, by radio frequency (RF) magnetron sputtering (JSP-8000, ULVAC, 450W RF power) of 20 nm thick Ti as an adhesion layer followed by 150 nm thick Au and Pt, respectively. A gold single crystal prepared by the Clavilier method[43] using a gold wire (99.999% pure, □= 1 mm, Tanaka Precious Metal) was used as a substrate for atomic force microscopic (AFM) measurements.

BNNTs donated by Dr. Golgberg of NIMS[44] were dispersed in IPA by sonicating with 3 mg/ml as initial concentration in an ultrasonic bath for 48 h. Liquid exfoliation method was used to obtain BNNS.[45-48] BN powder was sonicated in IPA with 3 mg/ml as initial concentration in an ultrasonic bath for 96 h. In both cases, the dispersions were centrifuged at 1500 rpm for 45 min after sonication and the 3/4 of supernatant was collected to be used for further measurements.[48]

Surface modification by BNNT and BNNS were carried out by spin coating of 5 µl of dispersion of BNNT on Au or 5 µl of dispersion of exfoliated BNNS on Au, Pt or glassy carbon (GC) substrate at 2000 rpm for 3 min and dried at 100 ºC for 30 min in an electronic furnace.

BN thin films[49,50] were deposited on the Au thin film and Au (111) single crystals by RF magnetron sputtering using a commercially available BN target (□= 4 inch, 99% purity, Jsputter) in Ar atmosphere (20 sccm) at room temperature with the substrate holder rotation rate of 10 rpm and the deposition rate of 0.1 Å/sec. Amount of deposited BN films were controlled by varying the deposition time; 50 sec, 100 sec, and 500 sec.

2.3 SEM, TEM, AFM and Electrochemical measurements

Scanning electron microscopy and high resolution transmission microscopy (HRTEM) were carried out with field emission scanning electron microscope (FE-SEM: S-4800, Hitachi) and by JEOL-JEM-2100F with power of 200 keV, respectively.

AFM measurements were performed by using Agilent 5500. For conducting AFM, Pt coated silicon nitride cantilever (PPP-FM, typical spring constant: 2.8 N/m, resonance frequency: 75 kHz, Nanosensors) was used.

Electrochemical measurements were carried out in a typical three electrode configuration. A Pt wire and a Ag/AgCl (sat. NaCl) electrodes were used as a counter and a reference electrode, respectively. A potentiostat/function generator (Hokuto Denko, HSV-100) and a speed control unit (Hokuto Denko, HR-202) were used to control the potential and the rotation speed of rotating disk electrode (RDE). All the electrochemical measurements were carried out in a 0.5 M H_2SO_4 an aqueous solution at room temperature. The electrolyte solution was saturated wi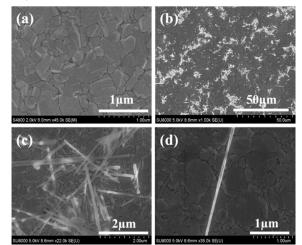th Ar or O_2 by passing the ultrapure Ar or ultrapure O_2 gas at least for 1 h to achieve an O_2 free or O_2 saturated condition before electrochemical measurements. The linear sweep voltammograms (LSVs) were recorded by varying the potential from 600 mV to -100mV with a scan rate of 10 mVs^{-1} and the rotaion speed was varied from 0 rpm to 3000 rpm. All electrodes were pre-treated by cycling the potential between -0.1 and +1.5 V in Ar saturated 0.5 M H_2SO_4 electrolyte solution at a sweep rate of 100 mVs^{-1} for 50 cycles to remove any surface contaminants before the ORR activity testing.

3. Results and Discussion

3.1 Gold electrode modified by BNNT and BNNS

Fig. 1 shows SEM images of (a) bare Au surface prepared by RF magnetron sputtering and (b-d) the Au surface spin coated with IPA dispersed BNNT. BNNTs were observed all over the Au surface with some aggregation. The width and length of BNNTs were in the order of 100 nm and a few µm, respectively, as shown in Fig. 1(d).

Fig. 1 SEM images of Au surface (a) without and (b-d) with spin coated dispersed BNNT.

Fig. 2 shows SEM images of the liquid exfoliated BNNS on Au substrate (a,b) and HRTEM images of BNNS (c, d). White spots in Fig. 2(a) correspond to BNNS, showing the uniform distribution of BNNS all over the Au surface. The size of exfoliated BNNS was in the order of few hundreds of nm in lateral dimension as revealed in enlarged SEM image (Fig. 2(b)). HRTEM images in Fig. 2(c, d) shows that the BNNS consists of a single to a few layers with honeycomb lattice structure (hexagonal atomic structure) and the fast Fourier transform (FFT) pattern shown as Fig. 2(c) inset confirms that BNNS is composed of hexagonal atomic structure. Zigzag and armchair edge structures are clearly observed in Fig. 2(c, d).[51] AFM measurements showed that the thickness of the deposited BNNS on Au was mono- to a few monolayers.[48]
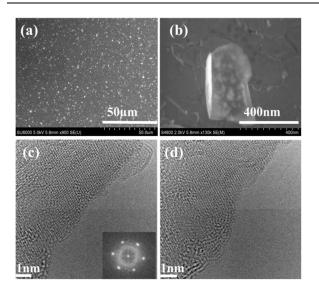
Fig. 2 (a, b) SEM images of liquid exfoliated BNNS spin coated on Au substrate and (c, d) HRTEM images of liquid exfoliated
5 BNNS. Inset of (c) is the FFT pattern of the image.

Fig. 3 shows the LSVs of gold electrode (a) without, (b) with IPA dispersed BNNT, and (c) with liquid exfoliated BNNS, measured in an O_2 saturated 0.5 M H_2SO_4 solution with the rotation rate between 0 and 3000 rpm. Potential was scanned
10 from +0.6 to -0.1V at the scan rate of 10mV/sec.

At the bare Au, cathodic current due to ORR started to flow at around +250 mV, increased as potential became more negative but no limiting current was observed in the potential region used in the present study.

15 At the BNNT coated Au, the cathodic current observed at around +350 mV and increased as potential became more negative but no limiting current was observed in the potential region used in the present study. It is clear that ORR activity was enhanced by BNNT modification. Further enhancement was
20 observed at the BNNS coated Au where the cathodic current started to flow at around +520 mV. In contrast to the bare Au and BNNT coated Au electrodes, the limiting current was observed at around +50 mV. Differences in the ORR activity can be seen more clearly in Fig. 3, which shows LSVs at (i) bare, (ii) BNNT
25 coated, and (iii) BNNs coated Au electrodes with the rotation rate of 1500 rpm. The potentials at which ORR current of -0.02 mA/cm^2 flowed was 0.22, 0.32, and 0.49V at the bare, BNNT coated, and BNNS coated Au electrodes, respectively. Although overpotential for ORR was reduced by both BNNT and BNNS
30 modifications, much larger effect was observed by BNNS modification (100 mV reduction by BNNT vs. 250 mV reduction by BNNS). This difference may be due to the very limited number of B- and/or N- edge structure in BNNT.[35] Theoretical calculations suggest the important role of edge structures as O_2
35 can be adsorbed in highly activated state at the edge of BN island.[48] As shown in Fig. 1, BNNT has very high aspect ratio with very low fraction of the edge compared with that of BNNS (Fig, 2), resulting in very small number of active sites at BNNT. Furthermore, poor contact of BNNT with Au surface may also
40 contribute to the lower activity as electronic communication between Au and BN is required to reduce O_2 and due to the curvature of BNNT, contact area and, therefore, the electronic communication of BNNT must be smaller than those of BNNS.
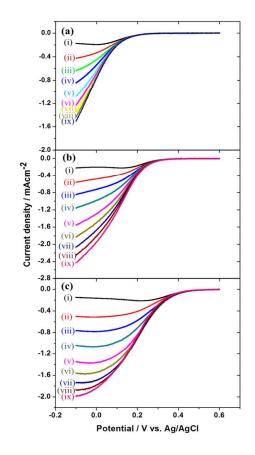
45

Fig. 3 LSVs of (a) bare, (b) BNNT modified, and (c) BNNS modified Au electrodes in O_2 saturated 0.5M H_2SO_4 solution in rotating disk electrode (RDE) configuration with rotation rate of (i) 0, (ii) 100, (iii) 250, (iv) 500, (v) 1000, (vi) 1500, (vii) 2000, (viii) 2500, and (ix) 3000 rpm. Sweep rate: 10 mV/s.
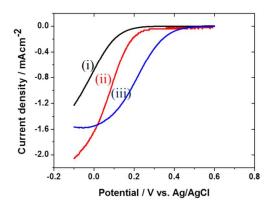

Fig. 4 LSVs of (i) bare, (ii) BNNT modified, and (iii) BNNS modified Au electrodes in O_2 saturated 0.5M H_2SO_4 solution in RDE configuration with rotation rate of 1500 rpm. Sweep rate: 10 mV/s.

50

3.2 Gold electrode modified by RF sputtered BN

To clarify the effects of contact between BN and Au and the thickness of BN, ORR activity of Au on which BN was sputter deposited was examined. Fig. 5 (a) shows the rotation rate dependent LSVs of Au coated with BN sputter deposited for (a) 50, (b) 100 and (c) 500 s in O_2 saturated 0.5M H_2SO_4 solution with various rotation rates. Potential was scanned from +0.6 to -0.1V. By comparing with the results at the bare Au shown in Fig. 3(a), it is clear that ORR activity was enhanced in all the cases. To compare the results easier, LSVs of (i) bare and BN sputter deposited Au electrodes with sputtering time of (ii) 50, (iii) 100 and (iv) 500 s with rotation rate of 1500 rpm were shown in Fig. 6. The potentials at which ORR current of -0.02 mA/cm^2 flowed was 0.37, 0.30, and 0.24V at Au electrodes with RF sputtered BN for 50, 100, and 500 s, respectively. They were more positive than that at the bare Au, which is 0.22V, by 0.15, 0.08, and 0.02 V. Thus, the ORR activity was less compared to those of BNNT and BNNS modified Au despite the expected better contact with Au substrate. The highest activity was observed when the deposition time was shortest, i.e., 50 s.
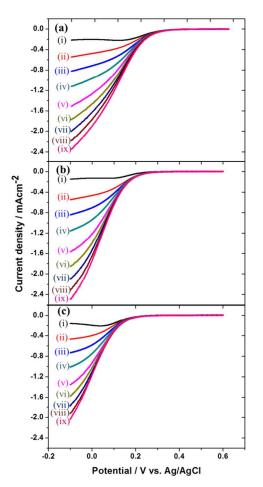

Fig. 6 LSVs of (i) bare and (ii – iv) BN sputter deposited Au electrode with sputtering time of (ii) 50, (iii) 100 and (iv) 500 s measured in O_2 saturated 0.5M H_2SO_4 solution in RDE configuration with rotation rate of 1500 rpm. Sweep rate: 10 mV/s.

Although we intended to deposit uniform BN films of 1, 2, and 10 nm thick by 50, 100, and 500 s deposition so that the thickness dependence of ORR activity can be studied quantitatively, BN nanoclusters of ca. 100 nm in diameter and 2-5 nm in height were deposited on Au surface as shown by AFM topography image in Fig. 7 regardless of deposition time.[52,53] As the deposition time increased, the sizes of BN nanoclusters did not change much but the number of the clusters increased. Current image shows that no current flowed on the the sputter deposited BN surface, showing it is insulating as BNNS.[48] Thus, ORR active site should be the edge of BN in this case as well and one expects the increase of active region and, therefore, ORR activity with the increase of the BN nanoclusters but experimental results showed other way round. Preparation of BN sputtered Au with much shorter deposition time and more careful surface analysis are under way to clarify the origin of deposition time dependence of ORR activity.

Fig. 7 (a) AFM topography and (b) conductance images of Au (111) surface on which BN was sputter deposited for 50 s.

3. 3 Quantitative comparison

For a more quantitative analysis, one needs to obtain the potential dependent rate constant of ORR. The current potential relations can be analyzed with the following Koutecky-Levich (K-L) equation:[54]

$$1/i = 1/i_k + 1/B\omega^{1/2} \qquad (1)$$
$$B = 0.620nFC_{O2}^{*}D^{2/3}v^{-1/6} \qquad (2)$$

where n is the number of electrons transferred in the overall reaction process, F is the Faraday constant (96490 C mol^{-1}), v is

Fig. 5 LSVs of Au electrode on which BN was sputter deposited for (a) 50, (b) 100 and (c) 500 s in O_2 saturated 0.5M H_2SO_4 solution in rotating disk electrode RDE configuration with rotation rate of (i) 0, (ii) 100, (iii) 250, (iv) 500, (v) 1000, (vi) 1500, (vii) 2000, (viii) 2500, and (ix) 3000 rpm. Sweep rate: 10 mV/s.
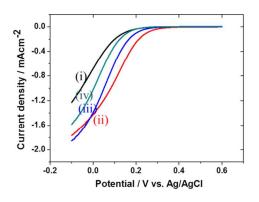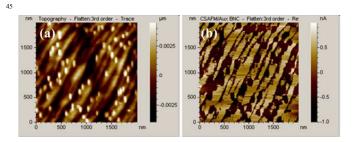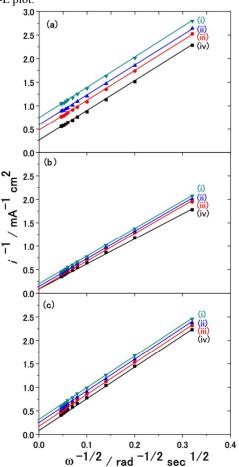
the kinematic viscosity $(0.01 cm^2 s^{-1})$,[55] D is the diffusion coefficient of oxygen molecule, C_{O2} is the bulk concentration of the oxygen $(1.1 \times 10^{-6} mol\ cm^{-3})$,[56,57] ω is the rotation rate, and i_k is the kinetic current without any mass transfer limitation, which is given by

$$i_k = nFAkC_{O2}^{*} \qquad (3)$$

Therefore, a linear plot of $1/i$ versus $1/\omega^{1/2}$ can be extrapolated to $1/\omega^{1/2} = 0$ to yield $1/i_k$. Then, the rate constant k can be obtained from equation (3).

Fig. 8 shows the K-L plots for the (a) bare, (b) BNNT modified, and (c) BNNS modified Au electrodes using the results of Fig. 3. Linear relations were observed in all cases and the number of electrons transferred (n) was calculated to be ca. 2 from the slopes of the K-L plots in all the cases, indicating that O_2 is reduced to hydrogen peroxide at these electrodes. The kinetic current, i_k, at a given potential can be obtained from the intercept of the K-L plot.

Fig. 8 Koutecky-Levich plots of (a) bare, (b) BNNT modified, and (c) BNNS modified Au electrodes in O_2 saturated 0.5M H_2SO_4 solution at (i) -0.02, (ii) -0.04, (iii) -0.06, and (iv) -0.10 V.

Tafel plots obtained from K-L plots are shown in Fig. 9. Single well-defined linear regions were observed at all electrodes except at the BNNS modified Au electrode where two well-defined linear regions were observed. The Tafel slopes and exchange current densities at bare, BNNT modified, BNNS modified, and BN sputter deposited (50, 100, 500 s) Au electrodes in O_2 saturated 0.5M H_2SO_4 solution are summarized in Table 1. The exchange current density at the BNNS modified Au electrode is 4 orders of magnitude higher than that at the bare Au electrode. The

slopes in low current density region are between -125 and -135 mV/dec at all electrodes except at the BNNS modified Au electrode where the slope is -72mV/dec. The slope at the BNNS modified Au electrode in high current region is -220 mV/dec. These results show that the ORR mechanism at the BNNS modified Au electrode is different from those at other electrodes. The Tafel slope at BNNS modified Au electrode in low current density region is close to that at Pt electrode in low current region, which is approximately -60mV/dec. Although more theoretical investigation is required to understand the unique behavior at the BNNS modified Au electrode, one plausible explanation is the presence of relative large O_2 adsorption sites at the edge of BNNS as the Tafel slope of -60mV/dec at Pt electrode in low current region is considered to be due to high coverage of adsorbed oxygenated intermediate species at Pt electrode.[58-60] The Tafel slopes observed at other electrodes are close to -120mV/dec, suggesting the first charge transfer step is the rate determining step.[61] Various values for the slope ranging from -120 mV/dec to over 200 mV/dec in higher current density region have been reported.[62-64] Very large Tafel slope at BNNS modified Au electrode in high current density region, -220 mV/dec, is not easy to be explained but transition from relatively small Tafel slope to very large slope should be relted to the slow turn over of adsorbed O_2 to the next step. Thus, the increase of active, i.e., O_2 adsorption, sites by using BNNS of much smaller dimension may increase ORR activity.
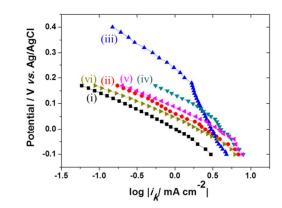

Fig. 9 Tafel plots of (i) bare, (ii) BNNT modified, (iii) BNNS modified, (iv) BN sputter deposited (50 s), (v) BN sputter deposited (100 s), and (vi) BN sputter deposited (500 s) Au electrodes in O_2 saturated 0.5M H_2SO_4 solution derived from the intercepts of K-L plots at various potentials.

Table 1 Kinetic parameters of various electrodes for ORR obtained from the results in Fig. 9.

Electrodes	Tafel slope (mV/decade)	Exchange current density (mA cm^{-2})
Bare Au	-125	6.31×10^{-8}
BNNT/Au	-130	1.99×10^{-6}
BNNS/Au	-136, -220	1.53×10^{-4}
Sputtered BN (50 s)/Au	-135	1.58×10^{-5}
Sputtered BN (100 s)/Au	-133	1.99×10^{-6}
Sputtered BN (500 s)/Au	-132	1.58×10^{-7}

3. 4 Effect of Substrate

Since theoretical calculations showed that BN-substrate interaction is the origin of the perturbation of electronic states of BN[48] and we briefly communicated that no enhancement of electrocatalytic activity for ORR was observed by BNNS modification at GC electrode,[48] substrate dependent ORR activities of BNNS were examined. Fig. 10 shows LSVs of (i) bare and (ii) BNNS modified Au electrodes, (iii) bare and (iv) BNNS modified Pt electrodes, and (v) bare and (vi) BNNS modified GC electrode in an O_2 saturated 0.5 M H_2SO_4 electrolyte solution at the rotation of 1500 rpm and the scan rate of 10mV/s. No change was observed by BNNS modification at GC electrodes (iii, iv) as already reported but current-potential relation at Pt electrode shifted negatively, i.e., ORR activity was reduced by the BNNS modification (v, vi), showing that BNNSs seem to block active Pt surface, which is one of the best ORR electrode.[2-4] These results confirm the importance of substrate in general and Au in particular. Theoretical study suggests that BN/Ni combination is a good candidate as an ORR electrocatalyst but low stability of Ni electrode in positive potential region prevents Ni to be used as a substrate. Search for more stable substrate is under way.
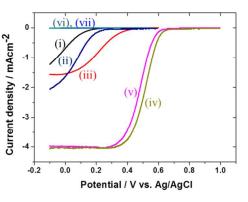

Fig. 10 LSVs of (i) bare, (ii) BNNT and (iii) BNNS modified Au, (iv) bare and (v) BNNS modified Pt, and (vi) bare and (vii) BNNS modified GC in O_2 saturated 0.5M H_2SO_4 solution at the rotation rate of 1500 rpm. Scan rate: 10mV/sec.

5. Conclusion

Electrocatalytic activities of various types of h-BN (BNNT, BNNS and sputter deposited BN) on gold for ORR were investigated in 0.5M H_2SO_4 solution. All BNs acted as ORR electrocatalyst and the overpotential for ORR at Au electrode was reduced by 20mV to 270 mV. The highest activity was obtained by BNNS modification and the reason for the enhanced catalytic activity of BNNS on Au was attributed to the presence of B- and/or N-edge structures. The kinetic parameters were determined and the difference in the Tafel slope at the BNNS modified Au electrode was noticed. While the BNNS modification was very effective to improve ORR activity at Au electrode, it has no and negative effects at GC and Pt electrodes, respectively, confirming the important role of the interaction between BN and Au for ORR activity enhancement.

Corresponding Author

e-mail: Kohei.UOSAKI@nims.go.jp

Notes and references

The authors declare no competing financial interests.

1. H.A. Gasteiger, N.M. Markovic, *Science* **2009**, *324*, 8-49.
2. M. Shao, K. Sasaki, R. Adzic, *J. Am. Chem. Soc.,* **2006**, *128*, 3526.
3. V. Stamenkovic, B. Fowler, B. Mun, G. Wang, P.Ross, C. Lucas, N. Markovic, *Science,* **2007**, *315*, 493.
4. E. H. Yu, K. Scott, R.W. Reeve, *Fuel Cells* **2003**, *3*, 169.
5. M. Winter, R. J. Brodd, Chem. Rev. 2004, *104*, 4245.
6. A. Kongkanand, S.Kuwabata, G. Girishkumar, P. Kamat, *Langmuir,* **2006**, *22*, 2392.
7. J. Zhang, K. Sasaki, E. Sutter, R. R. Adzic, *Science,* **2007**, *315*, 220.
8. B. Lim, M. J. Jiang, P. H. C. Camargo, E. C.Cho, J. Tao, X. M. Lu, Y. M. Zhu, Y. N. Xia, *Science,* **2009**, *324*, 1302.
9. F. Colmati, E. Antolini, E. R. Gonzalez, *J. Power Sources* **2006**, *157*, 98.
10. J. Zhang, H. Z. Yang, S. J. Y. Fang, H. Zou, *Nano Lett.,* **2010**, *10*, 638.
11. W. Chen, J. M. Kim, S. H. Sun, S. W. Chen, *J. Phys. Chem. C,* **2008**, *112*, 3891.
12. Y. Xu, H. Wang, R. Zhu, C. Liu, X. Wu, B. Zhang, *Chem. Asian J.,* **2013**, *8*, 1120.
13. G. Wu, P. Zeleny, *Acc. Chem. Res.,* **2013**, *46*, 1878.
14. X. Yu, S. Ye, *J. Power Sources,* **2007**, *172*, 145.
15. Y. Y. Shao, J. Liu, Y. Wang, Y. H. Lin, *J. Mater. Chem.,* **2009**, *19*, 46.
16. Y. J. Wang, D. P. Wilkinson, J. Zhang, *J. Chem. Rev.* **2011**, *111*, 7625.
17. B. Cao, G. M. Veith, R. E. Diaz, J. Liu, E. A. Stach, R. R. Adzic, P. G. Khalifah, *Angew. Chem. Int. Ed.* **2013**, *52*, 10753.
18. Y. Maekawa, A. Ishihara, J. H. Kim, S. Mitsushima, K.-i. Ota, *Electrochem. Solid-State Lett.* **2008,** *11*, B109-B112.
19. G. Zhong, H.Wang H. Yu, F.Peng, *Fuel Cells,* **2013**, *13*, 387.
20. R. L. Liu, D. Q. Wu, X. L. Feng, K. Mullen, *Angew. Chem., Int. Ed.,* **2010**, *49*, 2565.
21. Z. S. Wu, S. Yang, Y. Yi Sun, K. Parvez, X. L. Feng, K. Mullen, *J. Am. Chem. Soc.* **2012**, *134,* 9082.
22. R. A. Sidik, A. B. Anderson, N. P. Subramanian, S. P. Kumaraguru and B. N. Popov, *J. Phys. Chem. B*, **2006**,*110*, 1787.
23. J.-i. Ozaki, T. Anahara, N. Kimura and A. Oya, *Carbon*, **2006**, *44*, 3358.

24. K. P.Gong, F. Du, Z. H. Xia, M. Durstock, L. M. Dai, *Science* **2009**, *323*, 760.

25. X. Hu, Y. Wu, H. Li, Z. Zhang, *J. Phys. Chem. C*, **2010**, *114*, 9603.

26. S. Wang, E. Iyyamperumal, A. Roy, Y. Xue, D, Yu, L. Dai, *Angew. Chem.*, **2011**, 123, 11960; *Angew. Int. Ed.*, **2011**, *50*, 11756.

27. D. Yang, D. Bhattacharjya, S. Inamdar, J. Park, J. Yu, *J. Am. Chem. Soc.*, **2012**, *134*, 16127.

28. T. Ikeda, M. Boereo, S. H. Huang, K. Terakura, M. Oshima, J. Ozaki, S. Miyata, *J Phys Chem C.,* **2010**, *114*, 8933.

29. A. Lyalin, A. Nakayama, K. Uosaki, T. Taketsugu, *Phys. Chem. Chem. Phys*., **2013**, *15*, 2809.

30. V. L. Solozhenko, A. G. Lasarzenko, J. P. Petitet, A. V. Kanaev, *J. Phys. Chem. Solids*, **2001**, *62*, 1331 and references therein.

31. D. Golberg, Y. Bando, Y. Huang, T. Terao, M. Mitome, C. Tang, C. Zhi, *ACS Nano*, **2010**, *4*, 2979.

32. Y. Lin, J. W. Connell, *Nanoscale*, **2012**, *4*, 6908.

33. T. Oku, in *"Syntheses and Applications of Carbon Nanotubes and Their Composites"* ed. S. Suzuki, Chap. 5, **2013**, Intech.

34. Z. Liu1, Y. Gong, W. Zhou, L. Ma, J. Yu, J. C. Idrobo, J. Jung, A. H. MacDonald, R. Vajtai, J. Lou1, P. M. Ajayan, *Nature Commun.*, **2013**, *4*, 2541

35. H. Zheng, C. Zhi, Z. Zhang, X. Wei, X. Wang, W. Guo, Y. Bando, D. Golberg, *Nano Lett*., **2010**, *10*, 5049.

36. S. Azevedo, J. R. Kaschny, C. M. de Castilho, F. de Brito Mota, *Eur. Phys. J. B*, **2009**, *67*, 507.

37. A. Lyalin, A. Nakayama, K. Uosaki, T. Taketsugu, *J. Phys. Chem. C*, **2013**, *117*, 21359.

38. Yao, Z., Nie, H., Yang, Z., Zhou, X., Liu, Z., Huang, S., *Chem. Commun*. **2012**, *48*, 1027.

39. L. Britnell, R. V. Gorbachev, R. Jalil, B. D. Belle, F. Schedin, M. I. Katsnelson, L. Eaves, S. V. Morozov, A. S. Mayorov, N. M. R. Peres, A. H. Castro Neto, J. Leist, A. K. Geim, L. A. Ponomarenko and K. S. Novoselov, *Nano Lett*., **2012**,*12*, 1707.

40. R. Laskowski, P. Blaha and K. Schwarz, *Phys. Rev. B,* **2008**, 78, 045409.

41. M. Gao, A. Lyalin and T. Taketsugu, *J. Phys. Chem. C*, **2012**, *116*, 9054.

42. M. Gao, A. Lyalin, T. Taketsugu, *J. Chem, Phys.*, **2013**, *138*, 034701.

43. Clavilier, J., Faure, R.; Guinet, G., Durand, R., *J. Electroanaly. Chemistry* **1980,** *107*, 205

44. D. Golberg, Y. Bando, C.C. Tang, C. Y. Zhang, *Adv. Mater.*, **2007**, *19*, 2413 and references therein.

45. J. N. Coleman, M. Lotya, A. O'Neill, S. D. Bergin, P. J. King, U. Khan, K. Young, A. Gaucher, S. De, R. J. Smith, I. V. Shvets, S. K. Arora, G. Stanton, H. Y. Kim, K. Lee, G. T. Kim, G. S. Duesberg, T. Hallam, J. J. Boland, J. J. Wang, J. F. Donegan, J. C. Grunlan, G. Moriarty, A. Shmeliov, R. J. Nicholls, J. M. Perkins, E. M. Grieveson, K. Theuwissen, D. W. McComb, P. D. Nellist, V. Nicolosi, *Science* **2011**, *331*, 568.

46. T. Sainsbury, A. Satti, P. May, Z. Wang, I. McGoven, Y. K. Gun'ko, J. Coleman, *J. Am. Chem. Soc*. **2012**, *134*, 18758.

47. W. Q. Han, L. Wu, Y. Zhu, K. Watanabe, T. Taniguchi, *Appl. Phys. Lett*., **2008**, *93*, 223103.

48. K. Uosaki, G. Elumalai, H. Noguchi, T. Masuda, A. Lyalin, A. Nakayama, T. Taketsugu, submitted.

49. W. Gessler, J. Haupt, A. Hoffmann, P. N. Gibson, D. G. Rickerby, *Thin Solid Films*, **1991**, *199*, 113.

50. D. G. Rickerby, P. N. Gibbson, W. Gissler, J. Haupt, *Thin Solid Films*, **1992**, *209*, 155

51. N. Alem, R. Erni, C. Kisielowski, M. D. Rossell, W. Gannett, A. Zettl, *Phy. Rev. B*, **2009**, *80*, 155425.

52. P. Sutter, J. Lahiri, P. Zahl, B. Wang, E. Sutter, *Nano Lett.*, **2013**, *13*, 276.

53. Since BN clusters were not clearly observed in SEM images, AFM was used to observe BN clusters by using a flat Au(111) surface as a substrate.

54. A. J. Bard, L. R. Faulkner, "*Electrochemical Methods: Fundamentals and Applications*", 2nd Ed. **2000**, Wiley, New York.

55. M. Kullapere, G. Jurmann, T. T. Tennno, J. J. Paprotny, F. Mirkhalaf, K. Tammeveski, *J. Electroanal. Chem*., **2002**, *599*, 183.

56. K. E. Gubbins, R. D. J. Walker, *J. Electrochem. Soc.*, **1965**, *112*, 469.

57. R. E. Davis, G. L. Horvath, C. W. Tobias, *Electrochim. Acta*, **1967**, *12*, 287.

58. N. M. Markovic, H. A. Gasteiger, B. N. Grgur, P. N. Rose, *J. Electroanal. Chem*. **1999**, *467*, 157.

59. V. Stamenkovic, T. J. Schmidt, P. N. Ross, N. M. Markovic, *J. Electroanal. Chem*. **2003**, *554-555*, 191.

60. B. Liu, A. J. Bard, *J. Phys. Chem. B* **2002**, *106*, 12801.

61. R. R. Adzic, N. Strbac, N. Anastasijevic, *Mate. Chem. Phys*.**1989**, *22*, 349.

62. S. M. Park, S. Ho, S. Aruliah, M. F. Weber, C. A. Ward, R. D. Venter, S. J. Srinivasan, *J. Electrochem Soc*., **1986**, *133*, 1641.

63. Y. Kiros, *J. Electrochem. Soc*. **1996**, *143*, 2152.

64. E. H. Yu, K. Scott, R. W. Reeve, *Fuel cells* **2003**, *3*, 169.